Polyhedron 196 (2021) 115017

Contents lists available at ScienceDirect

Polyhedron

journal homepage: www.elsevier.com/locate/poly

A new series of Schiff base Ni(II)$_4$ cubanes: Evaluation of magnetic coupling via carboxylate bridges

Alexey N. Gusev [a], Ivan Nemec [b,c], Radovan Herchel [c], Yuriy I. Baluda [a], Mariya A. Kryukova [d], Nikolay N. Efimov [f], Mikhail A. Kiskin [f], Wolfgang Linert [e,*]

[a] Crimean Federal University, Simferopol 295007, Russia
[b] Central European Institute of Technology, CEITEC BUT, Technická 3058/10, Brno, Czech Republic
[c] Department of Inorganic Chemistry, Faculty of Science, Palacký University, 77147 Olomouc, Czech Republic
[d] Institute of Chemistry, Saint Petersburg State University, 198504 Saint Petersburg, Russia
[e] Institute for Applied Synthetic Chemistry, Vienna University of Technology, Getreidemarkt 9/163, A-1060 Vienna, Austria
[f] N.S. Kurnakov Institute of General and Inorganic Chemistry, Russian Academy of Sciences, Moscow 119991, Russia

ARTICLE INFO

Article history:
Received 27 October 2020
Accepted 28 December 2020
Available online 2 January 2021

Keywords:
Ni(II) complex
Schiff base
Cubane-like structures
X-ray diffraction
Magnetic properties

ABSTRACT

The Schiff base ligand H_2L has been synthesized by condensation of 2-aminophenol with 3-methyl-1-phenyl-4-formylpyrazol-5-one and reaction between H_2L and Ni(OOCR$_3$)$_2$, R = H in **1**, –CH$_3$ in **2**, Cl in **3**, yielded three new tetranuclear Ni(II) complexes. The complexes have been characterized by elemental analysis, IR- and ES-MS spectroscopy. Their structures as well as structure of ligand were determined by single-crystal X-ray diffraction. Compounds **1**–**3** possesses tetranuclear cubane-like structures containing $[Ni_4L_4(R_3COO)_2]^{2-}$ complex anions, which are charge balanced by two triethyl ammonium cations. Furthermore, the crystal structure of the Ni(II) cubane compound containing trichloroacetate bridging ligands, is reported for the first time. Variable temperature magnetic susceptibility measurements revealed interplay between ferromagnetic and antiferromagnetic exchange in the tetranuclear cubane-like compounds **1**–**3**, in which ferromagnetic interactions were enhanced by introducing carboxylate bridging groups. DFT calculations supported the analysis of magnetic data.

1. Introduction

Tetranuclear cubane-like M_4O_4 complexes including high-spin cobalt(II) and nickel(II) metal centers have been a very important class of molecules due to their potential application as a new type of magnetic materials [1,2]. The magnetic behavior of Co(II) and Ni(II) complexes with a cubane-like inner core, typically with Schiff base ligands, is very intriguing and depends on several structural factors. In general, the Ni_4O_4 cubane may exhibit either ferromagnetic or antiferromagnetic interactions among the nickel ions, depending upon the combination of the cubane topology and Ni-O-Ni angles. The structure of the cubane cores can be modified by introducing alterations in the coordinating ligands and the change in crystallization conditions such as solvent, temperature, guest molecules and pH [3–20]. This is apparently helpful for the synthesis of new molecular magnets allowing preparation of the Co(II) or Ni(II) cubanes with the dominant ferromagnetic interactions among the metal centers and non-negligible magnetic anisotropy of the ground state. Such compounds can exhibit slow relaxation of magnetization of molecular origin characteristic for Single-Molecule Magnets (SMMs) [3–6].

A great number of the cubane structures based on Schiff bases are formed on the basis of derivatives of salicylic aldehyde [3–20]. Such complexes are widely investigated due to the simplicity of their synthesis. Recently, we have started to develop new metal complexes based on polydentate Schiff-base ligands on 4-acylpyrazol-5-ones basis [21], which could be considered as a structural analog of salicylic aldehyde. In the present study, we have synthesized new Schiff-base ligand H_2L by the condensation of o-aminophenol with 3-methyl-1-phenyl-4-formylpyrazol-5-one (Scheme 1). We have also prepared three new cubane complexes by a reaction between H_2L and Ni(OOCR)$_2$·xH_2O (R = CH$_3$, (CH$_3$)$_3$C and CCl$_3$). The alteration of the carboxylate ligands was done in an attempt to modify the cubane structures and thus also the Ni-O-Ni exchange pathways. Furthermore, it must be stressed that trichloroacetate is a rather uncommon ligand in the nickel coordination compounds and its bridging function has been structurally confirmed only in a couple of compounds yet [22]. None of them possessed the cubane like structure and thus, here we present the first Ni cubane compound bridged by trichloroacetate ligand.

* Corresponding author.

https://doi.org/10.1016/j.poly.2020.115017
0277-5387/

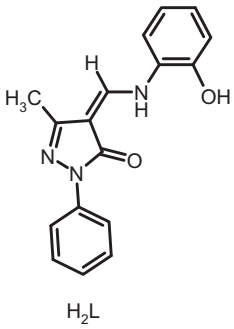

H_2L

Scheme 1. Structure of H_2L.

Moreover, we present a detailed magnetic study explaining the observed unexpected magnetic behavior of complexes in correlation to their structures.

2. Experimental

2.1. Materials and methods

All chemicals and solvents used for the synthesis were of analytical grade. 2-Aminophenol and $Ni(CH_3COO)_2{\cdot}4H_2O$ were commercially available and used as received without further purification. The starting nickel pivalate and trichloroacetate were synthesized according to known procedures [23]. The synthesis of new compounds was carried out with the use of trimethylacetic ant trichloracetic acid (Acros Organics). 3-methyl-1-phenyl-4-formylpyrazol-5-one was synthesized as described in the literature [24,25]. The purity and composition of the prepared complexes were confirmed by means of elemental analysis, electrospray-ionization mass-spectrometry (ESI–MS), and FT-IR spectroscopy, and single-crystal X-ray structure analysis.

Elemental analyses of C, H, and N were performed with a Perkin–Elmer 240 C analyzer. ^{1}H NMR spectra were recorded on a Bruker VXR-400 spectrometer at 400 MHz from solutions in DMSO-d^6. IR spectra were measured with a Spectrum Two PerkinElmer Inc spectrometer in the range 4000–400 cm^{-1}. Electrospray mass spectra of complexes were measured with the Finnagan TSQ 700 mass spectrometer in positive ion mode. Samples were prepared at a concentration of ~2 mg/ml MeOH. The mass spectra were acquired over the *m*/*z* range of 50–2000; several scans were averaged to provide the final spectrum.

Magnetic measurements were carried out on a SQUID MPMS 5S Quantum Design magnetometer in the 2–300 K temperature range. The diamagnetic contributions of the samples were estimated from Pascal's constants.

2.2. Synthesis

2.2.1. Syntheses of the Schiff base ligand

The ligand H_2L 4-*{[(2-hydroxyphenyl)amino]methylene}-5-methyl-2-phenyl-2,4-dihydro-3H-pyrazol-3-one* was prepared by the condensation of 2-aminophenol (0.546 g, 5 mmol) with 3-methyl-1-phenyl-4-formylpyrazol-5-one (1.01 g, 5 mmol) in presence of a single drop of glacial acetic acid in methanol medium (50 mL). On refluxing the methanolic solution for 5 h a light-yellow solid was obtained. Precipitate was filtered off and recrystallized from ethanol. Yield 1.55 g (87%).

Light-yellow crystals. Yield 84%. Anal. calc. for $C_{17}H_{15}N_3O_2$: C 69.61%, H 5.15%, N 14.33%. Found: C, 69.70; H, 5.22; N, 14.41%. IR spectrum, selected bands, cm^{-1}: 1668, 1623, 1593, 1488, 1317, 1270, 758, 688. ^{1}H NMR, d (ppm): 2.30 (3H, s, CH_3), 6.93 (H, d, *J* = 2.9 Hz) 7.05 (H, m, *J* = 3.2 Hz) 7.11 (H, m, *J* = 2.7 Hz) 7.18 (H, d, *J* = 2.9 Hz) 7.41 (2H, d, *J* = 2.5 Hz) 7.72 (H, d-d, *J* = 2.7 Hz), 7.99 (2H, d, *J* = 2.9 Hz), 8.70 (1H, d, *J* = 2.7 Hz, CH–NH), 10.53 (1H, s OH) 11.56 (1H, d, *J* = 2.7 Hz, CH–NH).

2.2.2. Coordination compounds

Synthesis of $(Et_3NH)_2[Ni_4L_4(CH_3COO)_2]{\cdot}\ CH_3COOH{\cdot}5H_2O$ (**1**).

$Ni(CH_3COO)_2{\cdot}4H_2O$ (0.248 g, 1 mmol) was added to 30 mL of a MeOH solution of the Schiff base ligand H_2L (0.293 g, 1 mmol). Et_3N (0.300 g, 2 mmol) was added to the resulting solution followed by further addition of 5 mL of MeOH. The resulting greenish-brown solution was stirred for 2 h and kept at room temperature for slow evaporation. Greenish-brown colour crystals appeared after 7 days.

Compound **1**. Yield 62 (%). Anal. Calc. for $C_{86}H_{106}N_{14}Ni_4O_{20}$ (%): C, 54.63; H, 5.65; N, 10.37. Found: C, 54.91; H, 5.58; N, 10.48%. IR (cm^{-1}): 3326(br), 3056(w), 2979(w), 1723(m), 1625(s), 1597(m), 1567(m), 1524(s), 1494 (s), 1353(s), 1334(s), 1247(s). ESI-MS: *m*/*z* 350.0450 [Ni(L)] + H^+] (Calcd 350.0239), *m*/*z* 699.0846 [$Ni_2(L)_2$] + H^+] (Calcd 699.0729).

Compounds $(Et_3NH)_2[Ni_4L_4(Me_3CCOO)_2]{\cdot}4H_2O$, (**2**) and $(Et_3NH)_2[Ni_4L_4(Cl_3CCOO)_2]{\cdot}2H_2O$, (**3**) were obtained in a similar manner using nickel(II) pivalate and nickel(II) trichloroacetate, respectively, instead of $Ni(CH_3COO)_2{\cdot}4H_2O$.

Compound **2**. Yield 75 (%). Anal. Calc. for $C_{90}H_{110}N_{14}Ni_4O_{16}$ (%): C, 57.54; H, 5.90; N, 10.44. Found: C, 57.38; H, 5.77; N, 10.32%. IR (cm^{-1}): 3310(br), 3056(w), 2980(w), 1626(s), 1599(m), 1522(m), 1500(s), 1352(s), 1331(s), 1246(s). ESI-MS: *m*/*z* 350.0438 [Ni(L)] + H^+] (Calcd 350.0239), *m*/*z* 699.0848 [$Ni_2(L)_2$] + H^+] (Calcd 699.0729).

Compound **3**. Yield 58 (%). Anal. Calc. for $C_{84}H_{88}Cl_6N_{14}Ni_4O_{14}$ (%): C, 51.34; H, 4.51; N, 10.82. Found: C, 51.62; H, 4.26; N, 10.72%. IR (cm^{-1}):): 3302(br), 3057(w), 2980(w), 1621(s), 1595 (m), 1519(s), 1499(s), 1354(s), 1339(s), 1238(s). ESI-MS: *m*/*z* 350.0440 [Ni(L)] + H^+] (Calcd 350.0239), *m*/*z* 699.0842 [$Ni_2(L)_2$] + H^+] (Calcd 699.0729).

2.3. X-ray crystallography

Diffraction data were collected using the standard rotational method on a Bruker SMART APEX II automated diffractometer equipped with a CCD detector and a monochromatic radiation source (H_2L, MoKα radiation, λ = 0.71073 Å) or a Bruker D8 Quest diffractometer equipped with a Photon 100 CMOS detector using the Mo-Kα radiation (compounds **1**–**2**) or a Super-Nova diffractometer equipped with a HyPix-3000 detector (Cu-Kα radiation λ = 1.54184 Å) (compound **3**). Data collection, data reduction, and cell parameters refinements were performed using the Bruker Apex III software package [26]. The molecular structures were solved by direct methods SHELXS-2014 and all non-hydrogen atoms were refined anisotropically on F^2 using full-matrix least-squares procedure SHELXL-2014 [27]. All hydrogen atoms were found in differential Fourier maps and their parameters were refined using a riding model with U_{iso}(H) = 1.2(CH) or 1.5(CH_3) U_{eq}. The crystallographic parameters and X-ray diffraction experimental parameters are given in Table S1. Non-routine aspects of refinement: The crystals of **2** and **3** suffer from solvent loss and therefore, despite numerous attempts, we were not able to get diffraction data of sufficient quality to reasonably model the electron density corresponding to triethylammonium cations and co-crystallized solvent molecules. However, the positions of the Et_3NH^+ cations in 2 and 3 were localized and the figures of the (approximate) second coordination spheres in these compounds are shown in supplementary. Prior the final refinement, a SQUEEZE procedure incorporated to PLATON was used to subtract the electronic density corresponding to cations and solvent molecules [28].

3. Results and discussion

New ligand H_2L was synthesized by the condensation of 2-aminophenol with the corresponding pyrazolone in refluxing anhydrous methanol and in the presence of a catalytic amount of acetic acid. An important aspect of this type of ligand is related to its tautomerism, both in the solid state and solution [29]. These molecules may exist in four tautomeric forms differing by the positions of the hydrogen atom, which could be located at the oxygen (imine-ol (form -A)), nitrogen (imine-one (form – B)), and carbon (imine-one (form – C)) atoms of the pyrazolone ring or at the azomethine N atom (amine-one) (form – D) – Scheme 2.

IR, ^{1}H NMR, and XRD data reveal that ketoamine tautomeric D – form predominates for the azomethines of H_2L both in solutions and in the solid state. Indeed. ^{1}H NMR spectra of H_2L (Fig. S1) demonstrate double signals of CH groups of the aminomethylene fragment =CH—NH— at 8.68 ppm a doublet of the NH-groups at 11.57 ppm. Moreover, IR spectra of H_2L show intense bands at 1668 cm^{-1} attributed to $\nu(C_{pyr}{=}O)$ vibrations (Fig. S3a). The crystal structure of H_2L was determined by single-crystal X-ray diffraction. H_2L1 crystallized in the orthorhombic space group $Pca2_1$. The structure of H_2L molecule is shown in Fig. 1. The crystallographic data are listed in Tables S1. The X-ray data on these compounds confirm that the present ligand exists in the amine-form.

3.1. Coordination compounds on the H_2L basis

The synthesis of **1**–**3** was carried out by reacting H_2L with the nickel carboxylates in methanol in presence of triethylamine as a base at ambient temperature. Detailed synthetic procedures are given in the experimental section. Complexes **1**–**3** were characterized by standard analytical/spectroscopic techniques and their solid-state structures were established by single-crystal X-ray diffraction analysis.

According to the element analysis data, these complexes possess Ni:L = 1:1 M ratio. ESI – mass spectroscopic data clearly suggests this ratio. Electrospray mass spectrum revealed a sequence of peaks corresponding to {NiL + H$^+$}, and {Ni_2L_2 + H$^+$} fragments with the correct isotopic spacings consistent with the charge (Fig. S2). ESI-data indicate that the tetranuclear cluster is fragile in solution and broke up under the conditions of the MS experiment

The infrared spectra for all complexes have been analyzed and compared with the free ligand spectrum (Fig. S3a-d). No stretching vibrations of the =CR—NH— fragments were found in IR-spectra of **1**–**3**, while the strong and sharp bands in the region of 1595–1599 cm^{-1} that can be assigned to the azomethine C=N stretching vibrations of the coordinated ligand were observed. A new intense absorption band, which is absent in the spectra of free ligand, appeared in the spectra of **1**–**3** with a maximum at 1352–1354 cm^{-1}. This could be assigned to C_{pyr}-O stretching vibrations confirming thus the formation of the imine-ole form of ligand upon coordination. Furthermore, two intense bands of the characteristic of the carboxylate-anion stretching are found in the regions 1621–1625 cm^{-1} and 1519–1524 cm^{-1}.

The crystal structures of **1**–**3** have been determined by X-ray single-crystal diffraction. Complexes **1**–**3** crystallizes in the monoclinic space groups $P2_1/c$ (**2**, **3**) and $P2_1/n$ (**1**). The crystallographic data are listed in Tables S1. The asymmetric unit of **1**–**3** contains anionic tetranuclear complex molecules and in the case of **1**, the positions of the triethylammonium cations, co-crystallized water and acetic acid molecules were determined. However, in **2** and **3**, the electron density outside of the complex anions was affected by partial solvent loss and thus it was not possible to be modeled reasonably and thus, it was removed using SQUEZZE procedure [28].

Molecular structures of complex anions are shown in Fig. 1. Complex anions exhibit distorted cubane topology of their coordination polyhedral in which the Ni(II) and the μ_3-O oxygen atoms occupy alternate vertices of the cube (Fig. 1). The Ni_4O_4 cubane cores are encapsulated by an organic shell of four Schiff base ligands (in double deprotonated form, L^{2-}) and two coordinated carboxylate-anions. Each Ni(II) atom is six-coordinated by five oxygen atoms and one imino nitrogen atom. Four out of five oxygen atoms originate from the Schiff base ligands and one is from the bridging carboxylate ligand. The H_2L ligand coordinates nickel atoms in a tridentate manner (the ONO atom donor set) by one imine nitrogen atom, oxygen atom from pyrazole ring and phenolate oxygen atom, which acts as μ_3-bridging atom. The metal–ligand bond lengths are very similar for both types of bonds, whereas the Ni-N bonds are a bit shorter than Ni-O bonds (Fig. 1). Remarkably, the longest bond lengths exceeding 2.10 Å are observed for some of the Ni-μ_3-O bonds.

Considering only the Ni_4O_4 cubane cores and the nature of the bridging ligands for the different faces of the cube, the D_{2d} symmetry could be assumed. The cubane cores are elongated and the Ni···Ni distances between the Ni atoms bridged by the carboxylate ligands (forming opposite faces of cubane) are shorter (e.g. 2.95–2.98 Å for **1**) than in four other faces (d(Ni···Ni) = 3.20–3.27 Å for **1**).

In crystal structure of **1**, the Et_3NH^+ cations are not linked to the complex anions by hydrogen bonding involving amine groups but remarkably, by weaker C—H···O hydrogen bonding (d(C···O) = 3.37–3.98 Å). The amine groups form rather strong N—H···O hydrogen bonds with co-crystallized water molecules (d(N···O) = 2.687(4) Å). These form O—H···O hydrogen bonds between the coordinated acetate ligands, other water molecules and non-coordinated mole-

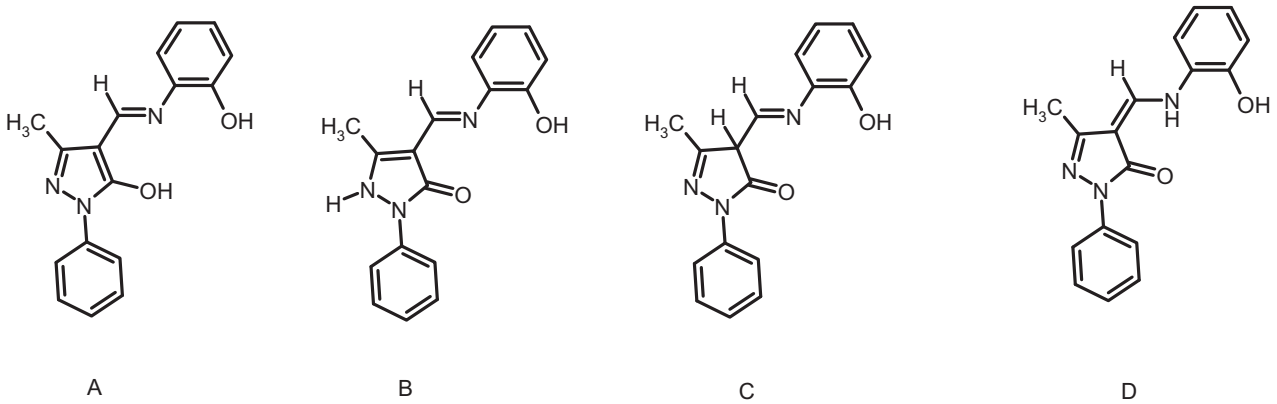

Scheme 2. Tautomeric forms of H_2L.

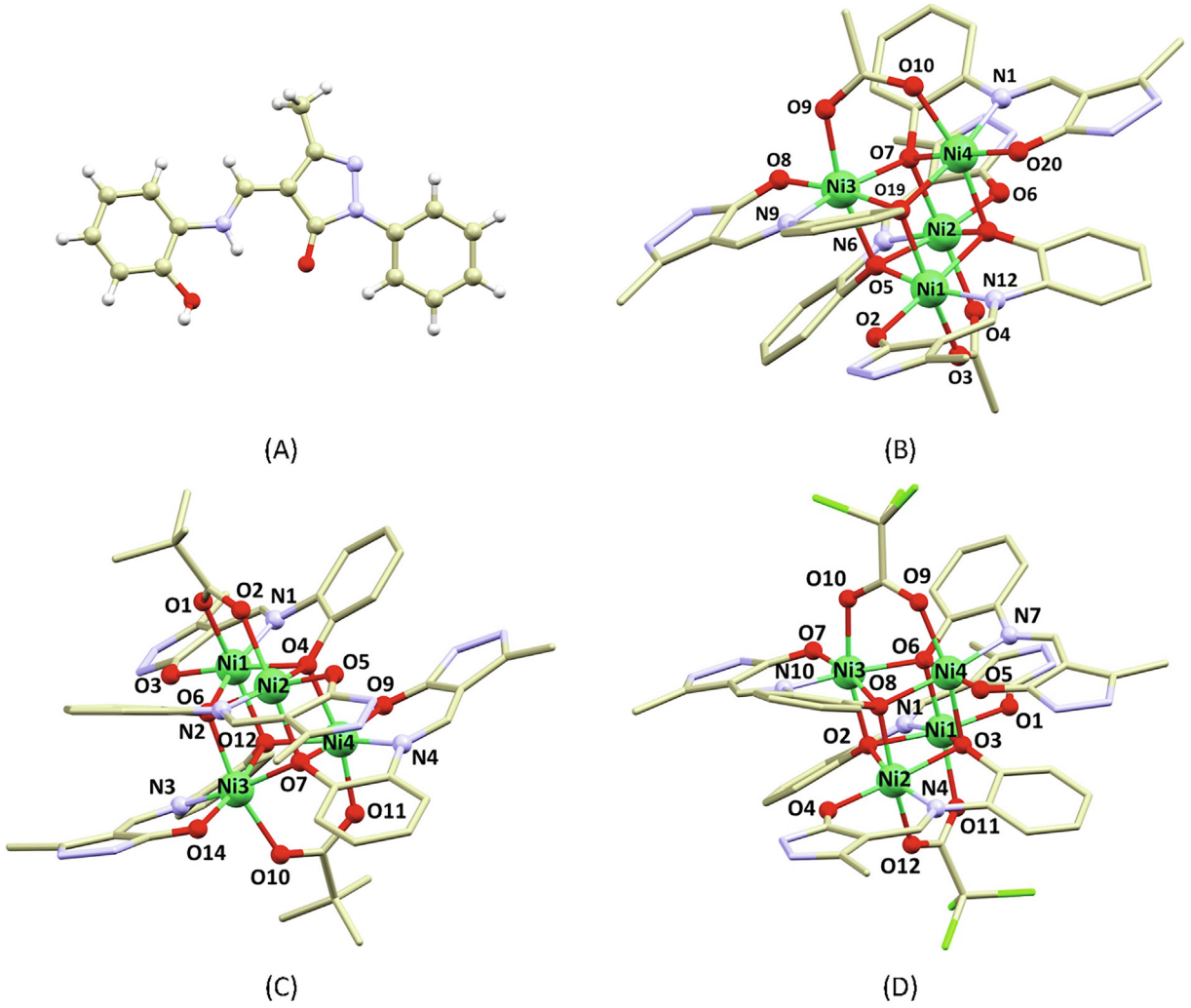

Fig. 1. Molecular structures of ligand H_2L (A) and tetranuclear complex molecules **1** (B), **2** (C) and **3** (D). In drawings of **1**–**3** the hydrogen atoms and phenyl rings (binding to pyrazol-3-one) were omitted for clarity. Selected bond lengths in the complex cations are listed in Table S2.

cules of acetic acid. Some of them provide non-covalent bridging between pyrazolone rings (O—H···N) and coordinated acetato ligands (non-covalent interactions are summarized in Supplementary Table S3).

In the case of crystal structures of **2** and **3**, the detailed discussion of the non-covalent interactions is prevented by a heavy disorder of the Et_3NH^+ cations and co-crystallized solvent molecules caused by the partial solvent loss. The positions of the cations and some of the solvent molecules can be located from difference maps and it can be concluded that in both compounds the present non-covalent interactions are similar to those observed in **1** with Et_3NH^+ cations forming N—H···O hydrogen bonds with co-crystallized water molecules (Fig. S5a and S5b). The noticeable difference is the absence of the co-crystallized acid molecule when compared to the crystal structure of **1**.

3.2. Magnetic properties

The thermal variation of the molar magnetization of **1**–**3** was measured over the range of 2–300 K and additionally, the magnetic

Table 1
The fitted spin Hamiltonian parameters for compounds **1**–**3**.

Compound	**1**		**2**		**3**	
J_{cb} (cm^{-1})	7.57	3.84	4.29	4.31	1.40	1.12
a_J	448	439	437	416	467	474
b_J	−4.47	−4.37	−4.34	−4.13	−4.67	−4.74
D (cm^{-1})	1.90	−10.8	10.6	−12.4	2.70	−3.33
g	2.32	2.34	2.30	2.29	2.12	2.12
RSS[a]	0.00110	0.00415	0.0638	0.501	0.0181	0.0268
J_{ph} derived values from linear equation $J_{ph} = a_J + <(Ni\text{-}O\text{-}Ni)_{av} \times b_J$						
J_{13} (cm^{-1})	−0.79	−0.18	−1.80	−1.75	−3.13	−3.14
J_{14} (cm^{-1})	−7.33	−6.60	−0.52	−0.53	−4.86	−4.90
J_{23} (cm^{-1})	−0.37	0.26	−1.67	−1.62	−1.42	−1.41
J_{24} (cm^{-1})	2.22	2.75	1.67	1.56	−0.77	−0.74

[a] RSS is residual sum of squares, $\sum_i \left(M_{mol,i}^{exp.} - M_{mol,i}^{calc.}\right)^2$.

field dependent isothermal magnetizations were acquired up to 5T. X-ray diffraction (XRD) measurements on the powder of **1**–**3** confirmed the retention of purity and crystallinity of related samples for magnetic measurement (Fig. S4 a–c).

The tetranuclear compounds **1**–**3** have the room temperature value of the effective magnetic moment in the 6–6.5 μ_B range, which corresponds to four magnetic centers with S = 1 having the g-factor slightly above free-electron value, which is typical for hexacoordinate Ni(II) ions [30]. At temperatures below 50 K, the increase of μ_{eff} is observed followed by its decrease on cooling to 2 K. Such behavior is most probably caused by the interplay of ferromagnetic and antiferromagnetic exchange interactions among Ni(II) ions influenced also by the single-ion zero-field splitting (ZFS). This complex situation is also reflected in the isothermal magnetization data, which does not follow Brillouin function and does not saturate at the maximal magnetic field.

Thus, the spin Hamiltonian comprising the isotropic exchange, ZFS and Zeeman term was postulated as follows

$$\hat{H} = -\sum_{k=1}^{3}\sum_{l=k+1}^{4} J_{kl}\left(\vec{S}_k \cdot \vec{S}_l\right) + \sum_{k=1}^{4} D_k\left(\hat{S}_{z,k}^2 - \hat{S}_k^2/3\right) + E_k\left(\hat{S}_{x,k}^2 - \hat{S}_{y,k}^2\right) + \mu_B B\sum_{k=1}^{4} g_k \hat{S}_{a,k} \quad (1)$$

where a-direction of the magnetic field is defined as $B_a = B(\sin(\theta)\cos(\varphi), \sin(\theta)\sin(\varphi), \cos(\theta))$ [31]. Such general spin Hamiltonian possesses too many free parameters and therefore the theoretical calculations at DFT level were performed to estimate the isotropic exchange parameters J_{kl} (*vide infra*). Furthermore, we assumed all ZFS parameters equal for the given tetranuclear compound and also the g-tensors were treated as isotropic. The DFT calculations showed that Ni(II) ions bridged also by the carboxylic groups pos-

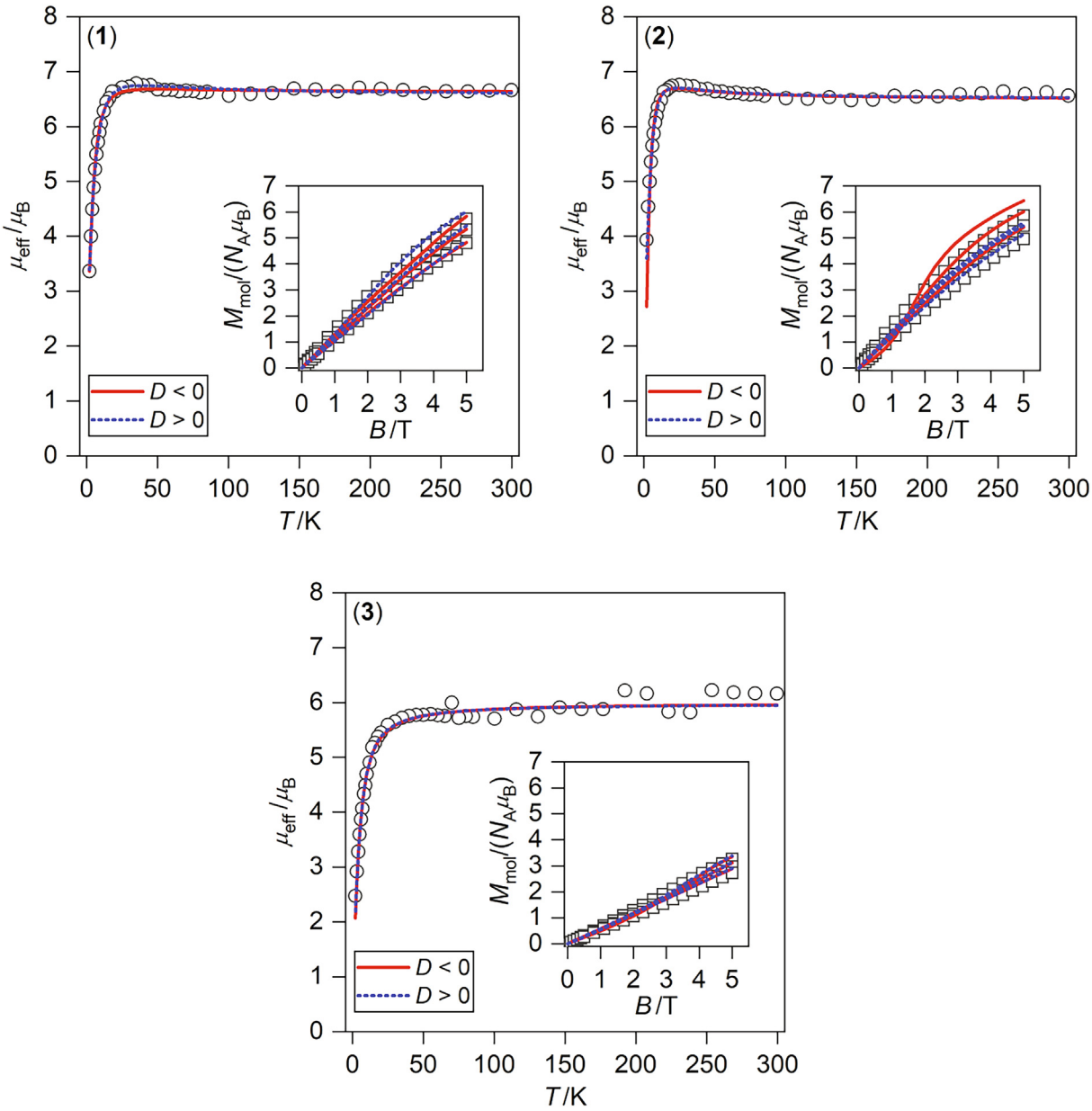

Fig. 2. Magnetic data for compounds **1**–**3**. Temperature dependence of the effective magnetic moment and the isothermal magnetizations measured at T = 2, 4, and 6 K. The empty circles represent the experimental data points and the lines represent the best fits calculated by using Eq. (1) with parameters listed in Table 1.

Table 2
The comparison of selected structural and magnetic parameters for dicarboxylato-bridged Ni_4O_4 cubanes.

CSD[a]	m-carboxylato	d(Ni-Ni) (Å)	<(Ni-O-Ni)$_{aver.}$	J_{cb} (cm^{-1})[b]	ref.
FOCXED	acetato	2.880	88.66	6.2	[35]
FOCXIH	acetato	2.879	88.51	12.0	
GIMBUC	acetato	2.906; 2.923	90.53; 91.38	5.5	[36]
GIMCAJ	propanoato	2.922; 2.911	91.54; 90.92	8.3	
HALCIJ	acetato	2.958	91.13	−4.06	[37]
HALCOP	propanoato	2.953	91.07	−5.16	
HALCUV	4-nitrobenzoato	2.959; 2.959	91.37; 91.61	−4.06	
IBOGAI	pivaloato	2.838; 2.907	87.68; 89.92	16.8[#]	[38]
LAWXUF	formato	3.037	93.70	−6.08	[38]
LAWYAM	2-chlorobenzoato	3.027	94.23	−3.08	
MUHLAE	pivaloato	2.922; 2.895	90.90; 90.51	11.4	[39]
TOPJEP	acetato	2.919; 2.907; 2.919; 2.929	91.32; 90.28; 90.35; 90.99	−9.64	[40]
TUFPEQ	acetato	2.889; 2.956	89.11; 90.51	−10.1	[41]
WIYVOQ	acetato	2.949; 2.947	90.54; 91.22	2.04	[42]
XIWFUG	trifluoroacetato	2.979; 2.962	93.60; 93.05	16.8[#]	[43]
XIWGAN	phenylacetato	2.937; 2.944	91.83; 92.42	14.4[#]	
1	acetato	2.948; 2.986	90.67; 91.93	7.57/3.84[#]	this work
2	pivaloato	2.964; 2.987	90.99; 91.68	4.29/4.31[#]	this work
3	trichloroacetato	2.982; 3.005	91.74; 92.63	1.40/1.12[#]	this work

[a] Cambridge Structural Database codes are used.
[b] J-values were scaled to spin Hamiltonian with $-J(S_1S_2)$ formulation.
[#] Means that also the zero-field splitting term was included in the analysis of magnetic properties.

sess ferromagnetic interactions (J_{cb}) and we assumed $J_{cb} = J_{12} = J_{34}$. Whereas other interactions mediated solely by phenolato groups are either weakly antiferromagnetic or weakly ferromagnetic (J_{ph}) and as expected, there is linear correlation between J_{ph} and average <(Ni-O-Ni) angle. Therefore, these J_{ph} (J_{13},J_{14},J_{23},J_{24}) were calculated during fitting procedure as $J_{kl} = a_J + b_J \times$<(Ni-O-Ni)$_{kl}$, which significantly reduced the number of varied parameters. We employed similar approach previously for analogous systems [3]. Next, both temperature and field-dependent data were fitted simultaneously for both possible signs of the D-parameters, and the best-fits results are summarized in Table 1 [32]. The better agreement with the experimental data was acquired for a positive value of D-parameters, and these fits are shown in Fig. 2. It is evident that the modification of bridging carboxylate acid led to a variation of both the isotropic exchange parameters and ZFS parameters – Table 1.

Next, the summary of similar Ni_4O_4 cubanes having octahedrally coordinated Ni atoms and two carboxylato-bridging ligands similarly to compounds **1**–**3** is presented in Table 2. First, it is obvious that various carboxylato ligands were already utilized in this part of the coordination chemistry, but this is first time when trichloroacetato ligand was used. Secondly, both antiferromagnetic and ferromagnetic exchange is reported for these carboxylato-bridging ligands ranging from −10 to +17 cm^{-1} and no clear correlation with selected structural parameters, like interatomic distance between two Ni atoms or average Ni-O-Ni angle, was found. Moreover, it must be pointed out that in all previously published results in Table 2, the authors used temperature dependent magnetic data (cT vs T) for analyzing magnetic properties. Furthermore, only in case of three compounds, magnetic data were analyzed together with ZFS terms. The fitted D-values were 3.1 cm^{-1} or −2.2 cm^{-1} for IBOGAI, 7.8 cm^{-1} for XIWFUG and 8.5 cm^{-1} for XIWGAN. However, even large values of $|D|$ up to 10–15 cm^{-1} can be expected for octahedral Ni(II) ions having the heterogenous coordination sphere and the large deviations from the ideal octahedron geometry [33,34]. To conclude, the nature of carboxylato bridging ligand has deep impact on the magnetic properties, albeit there is no obvious magneto-structural correlation.

3.3. DFT calculations

The complexity of the isotropic exchange interactions in **1**–**3** was assessed also by DFT calculations employing ORCA 4.2 ab initio computation package [44]. The respective molecular structures were extracted from the experimental X-ray data followed by the optimization of the hydrogen atom's positions with PBE functional [45]. Next, B3LYP functional [46] was utilized for the calculations of high-spin (HS) states and several broken-symmetry spin states (BS) in order to calculate individual J-parameters using Ruiz's approach [47]. In all calculations, def2-TZVP basis set was used for all atoms except for carbon and hydrogen atoms, for which def2-SVP basis set was used [48]. Moreover, RIJCOSX approximation [49] was used to speed up the calculations together with def2/J auxiliary basis set [50]. The calculations for **1**–**3** were based on the following spin Hamiltonian

$$\hat{H} = -J_{12}\left(\vec{S}_1 \cdot \vec{S}_2\right) - J_{13}\left(\vec{S}_1 \cdot \vec{S}_3\right) - J_{14}\left(\vec{S}_1 \cdot \vec{S}_4\right) - J_{23}\left(\vec{S}_2 \cdot \vec{S}_3\right) - J_{24}\left(\vec{S}_2 \cdot \vec{S}_4\right) - J_{34}\left(\vec{S}_3 \cdot \vec{S}_4\right) \quad (2)$$

and the values of the calculated J-parameters are listed in Table 3. An example of BS calculation for **3** is visualized in Fig. 3 [51]. Evidently, a relatively strong ferromagnetic exchange is triggered by the carboxylate-bridging ligands $OOCR_3$ and its strength is only slightly modified by the alternation of carboxylic groups. Comparison with isotropic exchange parameters (Table 1) determined from the experimental data shows that DFT calculations overestimates this type of the exchange. It is well-known that the isotropic exchange in Ni_4 cubane is dependent on Ni-O-Ni angle, [3–5,52] and also in this series of compounds **1**–**3**, the magneto-structural linear correlation can be established – Fig. 4.

Table 3
The calculated J-parameters for **1**–**3** using B3LYP functionals.

	1	**2**	**3**
J_{12}	10.0*	10.1*	10.6*
J_{13}	−0.11	−1.26	−0.17
J_{14}	−5.08	−2.28	−0.11
J_{23}	−0.36	−1.35	1.09
J_{24}	2.36	−0.76	3.60
J_{34}	11.2*	11.3*	10.9*

[a]Values of J-parameters are in cm^{-1}, the values marked with an asterisk correspond to superexchange pathways comprising also acetate group.

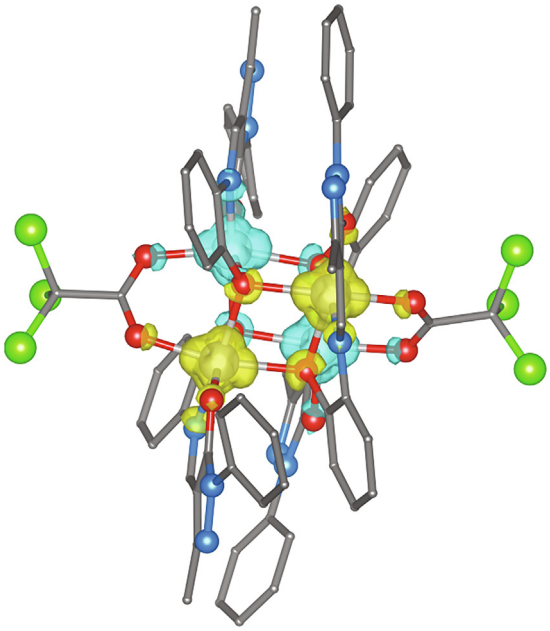

Fig. 3. The calculated spin density distribution using B3LYP of **3** for the BS12 state. Positive and negative spin density is represented by yellow and cyan surfaces, respectively. The isodensity surfaces are plotted with the cut-off value of $0.01ea_0^{-3}$. Hydrogen atoms are omitted for clarity.

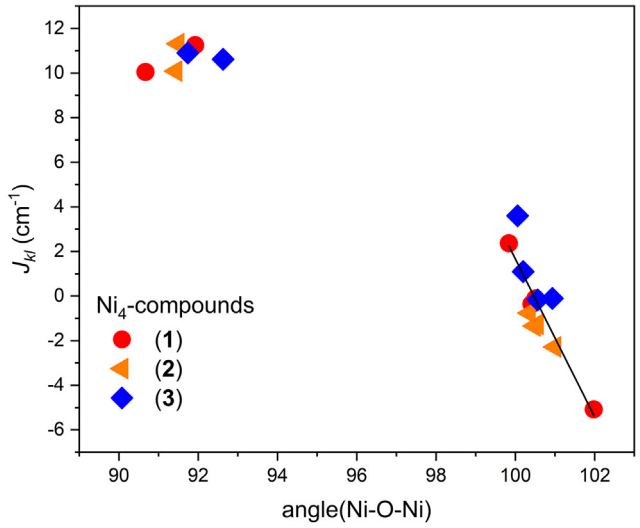

Fig. 4. The magneto-structural data for **1–3**, the dependence of DFT calculated J_{kl}-parameters on the average Ni–O–Ni angle. The full line corresponds to linear correlations for the isotropic exchange parameters for the superexchange pathways excluding carboxylate bridge with J/hc = 356–3.54×(Ni-O-Ni).

4. Conclusions

In summary, we have reported on the synthesis of three new cubane complexes **1–3** with were prepared by reactions between nickel carboxylates and Schiff base ligand H_2L. Determination of the crystal structures confirmed cubane-like structure with the {Ni$_4\mu^3$-O$_4$}cores, which are elongated having shorter Ni···Ni distances in the faces supported by carboxylate bridging ligands. Magnetic properties of **1–3** were measured using the SQUID magnetometer and by analysis of the data on spin Hamiltonian, it was revealed that dominant ferromagnetic interactions are transmitted via carboxylate bridges while the μ^3-O atoms mediate weak ferro- or antiferromagnetic exchange interactions. DFT calculations are in agreement with this model albeit predicted stronger ferromagnetic exchange interactions mediated by carboxylate ligands in **1–3**.

CRediT authorship contribution statement

Alexey N. Gusev: Investigation, Methodology, Funding acquisition, Writing - original draft. **Ivan Nemec:** Data curation, Formal analysis, Funding acquisition, Investigation, Methodology, Writing - original draft. **Radovan Herchel:** Data curation, Investigation, Methodology, Writing - original draft. **Yuriy I. Baluda:** Data curation, Investigation, Methodology. **Mariya A. Kryukova:** Data curation, Investigation. **Nikolay N. Efimov:** Data curation, Investigation. **Mikhail A. Kiskin:** Data curation, Investigation. **Wolfgang Linert:** Supervision, Writing - review & editing.

Declaration of Competing Interest

The authors declare that they have no known competing financial interests or personal relationships that could have appeared to influence the work reported in this paper.

Acknowledgments

The authors would like to acknowledge the financial support from the Russian Presidential grant (project № MD-1765.2019.3). The authors are also grateful Centre for X-ray Diffraction Studies of Research park of St. Petersburg State University for the help of some structural studies. R.H. and I.N. acknowledge the financial support from institutional sources of the Department of Inorganic Chemistry, Palacký University Olomouc, Czech Republic. I.N. acknowledges following projects: CEITEC 2020 (LQ1601), LO1305 and the ERC under the European Union's Horizon 2020 research and innovation programme (GA No 714850).

Appendix A. Supplementary data

CCDC 2039115-2039118 contain the supplementary crystallographic data for compounds H_2L and **1–3**, respectively. These data can be obtained, free of charge, via http://www.ccdc.cam.ac.uk/conts/retrieving.html, or from the Cambridge Crystallographic Data Centre, 12 Union Road, Cambridge CB2 1EZ, UK; fax: (+44) 1223-336-033; or e-mail: deposit@ccdc.cam.ac.uk. Supplementary data to this article can be found online at https://doi.org/10.1016/j.poly.2020.115017.

References

[1] A.K. Powell, in: Comprehensive Coordination Chemistry II, Pergamon, Oxford, 2003, p. 169.
[2] , Advances in Inorganic Chemistry vol. 43 (1995) 261.
[3] R. Herchel, I. Nemec, M. Machata, Z. Trávníček, Dalton Trans. 45 (2016) 18622.
[4] R. Herchel, I. Nemec, M. Machata, Z. Trávníček, New J. Chem. 41 (2017) 11258.
[5] M. Das, R. Herchel, Z. Trávníček, V. Bertolasi, D. Ray, New J. Chem. 42 (2018) 16717.
[6] M.A. Nadeem, M.C. Cin Ng, P. Jan van Leusen, J.A.S. Kçgerler, Chem. Eur. J. 26 (2020) 7589.
[7] L.B.L. Escobar, G.P. Guedes, S. Soriano, J. Marbey, S. Hill, M.A. Novak, M.G.F. Vaz, Inorg. Chem. 58 (2019) 14420.
[8] S.-H. Zhang, Y.D. Zhang, H.H. Zou, J.J. Guo, H.P. Li, Y. Song, H. Liang, Inorg. Chim. Acta 396 (2013) 119.
[9] A. Das, F.J. Klinke, S. Demeshko, S. Meyer, S. Dechert, F. Meyer, Inorg. Chem. 51 (2012) 8141.
[10] S.-H. Zhang, N. Li, C.-M. Ge, C. Feng, L.-F. Ma, Dalton Trans. 40 (2011) 3000.
[11] S. Karmakar, S. Khanra, CrystEngComm 16 (2014) 2371.
[12] D. Mandal, C.S. Hong, H.C. Kim, H.-K. Fun, D. Ray, Polyhedron 27 (2008) 2372.
[13] F. Torić, G. Pavlović, D. Pajić, M. Cindrić, K. Zadro, CrystEngComm 20 (2018) 3917.
[14] Z. You, Y. Luo, S. Herringer, Y. Li, S. Decurtins, K.W. Krämer, S.-X. Liu, Crystals 10 (2020) 592.

[15] S. Saha, S. Pal, C.J. Gómez-García, J.M. Clemente-Juan, K. Harms, H.P. Nayek, Polyhedron 74 (2014) 1.
[16] S.-Y. Lin, G.-F. Xu, L. Zhao, Y.-N. Guo, J. Tang, Q.-L. Wang, G.-X. Liu, Inorg. Chim. Acta 373 (2011) 173.
[17] L. Botana, J. Ruiz, A.J. Mota, A. Rodriguez-Dieguez, J.M. Seco, I. Oyarzabal, E. Colacio, Dalton Trans. 43 (2014) 13509.
[18] S.-Y. Zhang, W.-Q. Chen, B. Hu, Y.-M. Chen, W. Li, Y. Li, Inorg. Chem. Commun. 16 (2012) 74.
[19] S. Liu, S. Wang, F. Cao, H. Fu, D. Li, J. Dou, RSC Adv. 2 (2012) 1310.
[20] S. Shit, M. Nandy, G. Rosair, C.J. Gómez-García, J.J. Borras Almenar, S. Mitra, Polyhedron 61 (2013) 73.
[21] a) A.N. Gusev, M.A. Kiskin, E.V. Braga, M. Chapran, G. Wiosna-Salyga, G.V. Baryshnikov, V.A. Minaeva, B.F. Minaev, K. Ivaniuk, P. Stakhira, H. Ågren, W. Linert, J. Phys. Chem. C 123 (2019) 11850;
b) A.N. Gusev, V.F. Shul'gin, E.V. Braga, I. Nemec, B.F. Minaev, G.V. Baryshnikov, Z. Trávníček, H. Ågren, I.L. Eremenko, K.A. Lyssenko, W. Linert, Polyhedron 155 (2018) 202.
[22] (a) L. Chen, X.-W. Wang, J.-Z. Chen, Jian-Hong Liu, Z. Naturforsch. 62b (2007) 1271;
(b) N. Dong, H. Wang, R.J. Barton, B.E. Robertson, J. Coord. Chem. 22 (1990) 191.
[23] (a) I.G. Fomina, G.G. Aleksandrov, Z.V. Dobrokhotova, O.Y. Proshenkina, M.A. Kiskin, Y.A. Velikodnyi, V.N. Ikorskii, V.M. Novotortsev, I.L. Eremenko, Russ. Chem. Bull., Int. Ed. 55 (2006) 1909;
(b) I.G. Fomina, Z.V. Dobrokhotova, G.G. Aleksandrov, O.Y. Proshenkina, M.L. Kovba, A.S. Bogomyakov, V.N. Ikorskii, V.M. Novotortsev, I.L. Eremenko, Russ. Chem. Bull. Int.Ed. 58 (2009) 11.
[24] Y.a. Kvitko, B.A. Porai-Koshits, Z.h. Org, Khim. 34 (1964) 3005.
[25] M. Shi, F. Li, T. Yi, D. Zhang, H. Hu, C. Huang, Inorg. Chem. 44 (2005) 8929.
[26] Bruker. Apex3, Bruker AXS Inc., Madison, Wisconsin, USA, 2015.
[27] G.M. Sheldrick, Acta Crystallogr, Sect. C, Struct. Chem. 71 (2015) 3.
[28] (a) A.L. Spek, Acta Cryst. E76 (2020) 1;
(b) A.L. Spek, Acta Crystallogr. Sect. C Struct. Chem. 71 (2015) 9–18.
[29] F. Marchetti, C. Pettinari, C. Di Nicola, A. Tombesi, R. Pettinari, Coord. Chem. Reviews 401 (2019) 213069.
[30] R.L. Carlin, Magnetochemistry, Springer, 1986.
[31] R. Boča, Theoretical Foundations of Molecular Magnetism, Elsevier, Amsterdam, The Netherlands, 1999.
[32] R. Boča, R. Herchel, Program POLYMAGNET 2006-2020.
[33] J. Titiš, R. Boča, Magnetostructural D correlation in Nickel(II) complexes: reinvestigation of the zero-field splitting, Inorg. Chem. 49 (2010) 3971.
[34] R. Boča, Zero-field splitting in metal complexes, Coord. Chem. Rev. 248 (2004) 757–815.
[35] J. Mayans, A.A. Athanasopoulou, A.T. Pham, M. Font-Bardia, E.C. Mazarakio-ti, M. Pilkington, T.C. Stamatatos, A. Escuer, Ni4 Cubanes from enantiomeri-cally pure 2-(1-hydroxyethyl)pyridine ligands: supramolecular chirality, Dalton Trans. 48 (2019) 10427.
[36] M. Das, R. Herchel, Z. Trávníček, V. Bertolasi, D. Ray, Anion coordination directed synthesis patterns for [Ni4] aggregates: structural changes for thiocyanate coordination and ligand arm hydrolysis, New J. Chem. 42 (2018) 16717.
[37] K. Chattopadhyay, G.A. Craig, A. Kundu, V. Bertolasi, M. Murrie, D. Ray, Hydroxido-supported and carboxylato bridge-driven aggregation for discrete [Ni 4] and interconnected [Ni 2]n complexes, Inorg. Chem. 55 (2016) 10783.
[38] G. Chaboussant, R. Basler, H.-U. Güdel, S. Ochsenbein, A. Parkin, S. Parsons, G. Rajaraman, A. Sieber, A.A. Smith, G.A. Timco, R.E.P. Winpenny, Nickel pivalate complexes: structural variations and magnetic susceptibility and inelas-tic neutron scattering studies, Dalt. Trans. (2004) 2758.
[39] M. Pait, A. Bauzá, A. Frontera, E. Colacio, D. Ray, A new family of Ni4 and Ni6 aggregates from the self-assembly of [Ni2] building units: role of car-boxylate and carbonate bridges, Inorg. Chem. 54 (2015) 4709.
[40] M.S. Jana, J.L. Priego, R. Jiménez-Aparicio, T.K. Mondal, Novel tetranuclear Ni(II) Schiff base complex containing Ni4O4 cubane core: synthesis, X-ray structure, spectra and magnetic properties, Spectrochim, Acta Part A Mol. Bio-mol. Spectrosc. 133 (2014) 714.
[41] C.G. Efthymiou, C. Papatriantafyllopoulou, N.I. Alexopoulou, C.P. Rap-topoulou, R. Boča, J. Mrozinski, E.G. Bakalbassis, S.P. Perlepes, A mononucle-ar complex and a cubane cluster from the initial use of 2-(hydroxymethyl)pyridine in nickel(II) carboxylate chemistry, Polyhedron 28 (2009) 3373.
[42] S. Akine, A. Akimoto, T. Shiga, H. Oshio, T. Nabeshima, Synthesis, stability, and complexation behavior of isolable salen-type N2S2 and N2SO ligands based on thiol and oxime functionalities, Inorg. Chem. 47 (2008) 875.
[43] A.K. Ghosh, M. Shatruk, V. Bertolasi, K. Pramanik, D. Ray, Self-assembled tetra- and pentanuclear nickel(II) aggregates from phenoxido-based ligand-bound Ni2 fragments: carboxylate bridge controlled structures, Inorg. Chem. 52 (2013) 13894.
[44] F. Neese, Wiley Interdiscip. Rev.: Comput. Mol. Sci. 8 (2018) e1327.
[45] J.P. Perdew, K. Burke, M. Ernzerhof, Phys. Rev. Lett. 77 (1996) 3865.
[46] (a) A.D. Becke, Phys. Rev. A 38 (1988) 3098;
(b) C. Lee, W. Yang, R.G. Parr, Phys. Rev. B 37 (1988) 785;
(c) P.J. Stephens, F.J. Devlin, C.F. Chabalowski, M.J. Frisch, J. Phys. Chem. 98 (1994) 11623.
[47] (a) E. Ruiz, J. Cano, S. Alvarez, P. Alemany, J. Comput. Chem. 20 (1999) 1391;
(b) E. Ruiz, A. Rodríguez-Fortea, J. Cano, S. Alvarez, P. Alemany, J. Comput. Chem. 24 (2003) 982.
[48] F. Weigend, R. Ahlrichs, Phys. Chem. Chem. Phys. 7 (2005) 3297.
[49] (a) F. Neese, F. Wennmohs, A. Hansen, U. Becker, Chem. Phys. 356 (2009) 98;
(b) R. Izsak, F. Neese, J. Chem. Phys. 135 (2011) 144105.
[50] F. Weigend, Phys. Chem. Chem. Phys. 8 (2006) 1057.
[51] K. Momma, F. Izumi, J. Appl. Crystallogr. 44 (2011) 1272.
[52] (a) M.A. Halcrow, J.-S. Sun, J.C. Huffman, G. Christou, Inorg. Chem. 34 (1995) 4167;
(b) A. Das, F.J. Klinke, S. Demeshko, S. Meyer, S. Dechert, F. Meyer, Inorg. Chem. 51 (2012) 8141.